Homogeneous Catalytic Carbonylation of Nitroaromatics. 8. Kinetic and Mechanistic Studies of the Carbon–Nitrogen Bond and Product Forming Steps from Ru(Ph₂PCH₂CH₂PPh₂)(CO)₂[C(O)OCH₃]₂: The Turnover Limiting Reactions in the Catalytic Cycle

Jerry D. Gargulak and Wayne L. Gladfelter*

Contribution from the Department of Chemistry, University of Minnesota, Minneapolis, Minnesota 55455

Received November 8, 1993[®]

Abstract: Mechanistic studies of the reaction of (*OC*-6-32)-dicarbonylbis(methoxycarbonyl)[1,2-bis(diphenylphosphino)-ethane]ruthenium(II) with *p*-toluidine to form *N,N'*-di-*p*-tolylurea are presented. The overall reaction was studied from 22 to 103 °C and was found to be first order with respect to each reactant. Spectroscopic and kinetic studies between 22 and 52 °C showed that the reaction proceeds through a species, Ru(dppe)(CO)₂[C(O)OCH₃][C(O)-NH(*p*-tolyl)], which is in equilibrium with Ru(dppe)(CO)₂[C(O)OCH₃]₂. The mechanism of the C–N bond forming step is proposed to involve nucleophilic attack on a coordinated Ru–CO moiety with subsequent cleavage of the C(O)–OMe bond. The methoxycarbonyl–carbamoyl complex decomposes in a unimolecular fashion to liberate CH₃OH, the starting catalyst Ru(dppe)(CO)₃, and *p*-tolyl isocyanate, which is immediately scavenged by excess amine to form *N,N'*-di-*p*-tolylurea. Studies of the analogous bis(isopropylcarbamoyl) complex provided supporting evidence for isocyanate elimination. Thermolysis of (*OC*-6-32)-dicarbonylbis(isopropylcarbamoyl)[1,2-bis(diphenylphosphino)-ethane]ruthenium(II) yields isopropylamine, the starting catalyst Ru(dppe)(CO)₃, and isopropyl isocyanate, which reacts with isopropylamine over time to form diisopropylurea. The kinetics obtained from all of the stoichiometric reactions were combined into a suitable expression and found to lie on the same Arrhenius activation energy plot as the overall rate of the catalytic reaction.

Introduction

The search for environmentally benign processes to replace the use of phosgene (Cl₂CO) for the production of isocyanates has focused attention on the homogeneous catalytic carbonylation of nitroaromatics.[1] When conducted in alcohols, the product is a carbamate (eq 1) and the catalysts, typically ruthenium, palladium, or rhodium, exhibit improved turnover rates and lifetimes.[2–9]

$$ArNO_2 + 3CO + CH_3OH \rightarrow ArNHC(O)OCH_3 + 2CO_2$$
$$(1)$$
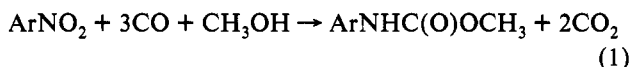
In our previous work[10–12] on the catalyst system developed by Grate and co-workers,[3–6] it was proposed that the monomeric catalyst Ru(dppe)(CO)₃ (**1**) (Chart 1), reacted rapidly with nitroaromatics to form the intermediate metallacycle Ru(dppe)-(CO)₂[C(O)N(Ar)O] (**2**). Similar metallacyclic structures have been identified in related reactions of palladium[13] and rhodium.[14] Methanol reacted with **2** to form the bis(methoxycarbonyl) complexes Ru(dppe)(CO)₂[C(O)OCH₃]₂ (**3** and **3'**), whose reaction with aromatic amines (eq 2) was proposed to be the rate

$$Ru(dppe)(CO)_2[C(O)OCH_3]_2 + ArNH_2 \rightarrow$$
$$Ru(dppe)(CO)_3 + ArNHC(O)OCH_3 + CH_3OH \quad (2)$$
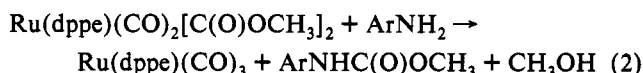
limiting step of the catalysis.[12] This paper will describe the studies of the reactivity of Ru(dppe)(CO)₂[C(O)OCH₃]₂ with aryl amines and the relationship this has to the mechanism of the catalytic carbonylation of nitroaromatics.

Experimental Section

General Procedure. Standard Schlenk techniques were implemented when working with all organometallic compounds, unless otherwise stated. A nitrogen-filled Vacuum Atmospheres glovebox equipped with a Dri-Train Model 40-1 inert gas purifier was employed for manipulations carried out under glovebox conditions. NMR spectroscopic work was performed on a Varian-Unity 300 instrument, and infrared spectra were collected on a Mattson Polaris spectrometer. Solution gas chromatography samples were analyzed on an HP 5890 Series II employing a 10-m megabor FFAP-cross-linked column and a flame ionization detector.

All chemicals, including anhydrous methanol packed under nitrogen, were purchased from Aldrich Chemical Co., except Ru₃(CO)₁₂ and dppe (1,2-bis[diphenylphosphino]ethane), which were purchased from Strem Chemical. Toluene, diethyl ether, and hexane were freshly distilled from benzophenone ketyl under nitrogen. Methylene chloride was distilled

[®] Abstract published in *Advance ACS Abstracts,* April 1, 1994.

(1) Cenini, S.; Pizzotti, M.; Crotti, C. In *Aspects of Homogeneous Catalysis;* Ugo, R., Ed.; Reidel: Dordrecht, 1988; Vol. 6, p 97.

(2) Cenini, S.; Pizzotti, M.; Crotti, C.; Porta, F.; La Monica, G. *J. Chem. Soc., Chem. Commun.* **1984,** 1286.

(3) Grate, J. H.; Hamm, D. R.; Valentine, D. H. U.S. Patent 4600793, 1986.

(4) Grate, J. H.; Hamm, D. R.; Valentine, D. H. U.S. Patent 4603216, 1986.

(5) Grate, J. H.; Hamm, D. R.; Valentine, D. H. U.S. Patent 4629804, 1986.

(6) Grate, J. H.; Hamm, D. R.; Valentine, D. H. U.S. Patent 4705883, 1987.

(7) Cenini, S.; Crotti, C.; Pizzotti, M.; Porta, F. *J. Org. Chem.* **1988,** *53,* 1243.

(8) Cenini, S.; Pizzotti, M.; Crotti, C.; Ragaini, F.; Porta, F. *J. Mol. Catal.* **1988,** *49,* 59.

(9) Cenini, S.; Ragaini, F.; Pizzotti, M.; Porta, F.; Mestroni, G.; Alessio, E. *J. Mol. Catal.* **1991,** *64,* 179.

(10) Kunin, A. J.; Noirot, M. D.; Gladfelter, W. L. *J. Am. Chem. Soc.* **1989,** *111,* 2739.
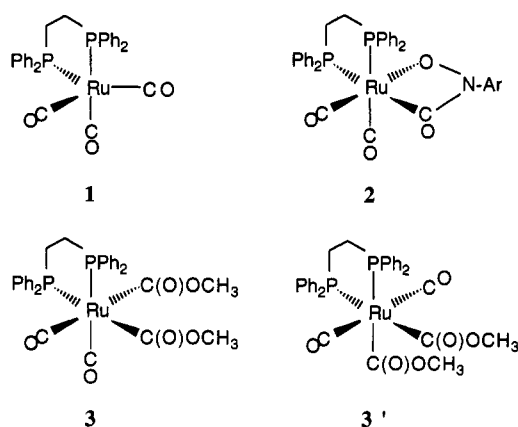
(11) Gargulak, J. D.; Noirot, M. D.; Gladfelter, W. L. *J. Am. Chem. Soc.* **1991,** *113,* 1054.

(12) Gargulak, J. D.; Berry, A. J.; Noirot, M. D.; Gladfelter, W. L. *J. Am. Chem. Soc.* **1992,** *114,* 8933.

(13) Leconte, P.; Metz, F.; Mortreux, A.; Osborn, J. A.; Paul, F.; Petit, F.; Pillot, A. *J. Chem. Soc., Chem. Commun.* **1990,** 1616.

(14) Ragaini, F.; Cenini, S.; Demartin, F. *J. Chem. Soc., Chem. Commun.* **1992,** 1467.

Chart 1. Structures of Intermediates in the Catalytic Cycle

Table 1. Rate Constants for the Reaction of Ru(dppe)(CO)₂[C(O)OCH₃]₂ with *p*-Toluidine between 75 and 103 °C

temp (°C)[a]	k_u[b]	[ArNH₂][c]	[Ru][d]
103.0[e]	0.50	0.15	22.9
103.0[e]	0.52	0.21	35.1
103.0[e]	0.54	0.36	26.4
95.0	0.44	0.20	29.7
95.0	0.40	0.11	29.7
95.0	0.43	0.86	29.7
95.0	0.40	0.14	29.7
95.0	0.41	0.14	14.8
95.0	0.41	0.14	44.5
91.5	0.30	0.45	26
85.0	0.18	0.28	18.6
75.0	0.068	0.19	29.7

[a] All reactions performed in the NMR spectrometer except where indicated. [b] Units are M⁻¹ min⁻¹. [c] Units are M. [d] Units are mM. [e] Reactions performed in an external constant temperature bath.

from calcium hydride. Compounds 1,[15] 3,[12,16] and Ru(dppe)(CO)₂[C(O)-NHCH(CH₃)₂]₂ (6)[17] were prepared as previously described. Carbon monoxide-¹³C in glass vessels and lecture bottles was purchased from Isotech. Throughout the paper, use of 3 or 3′ refers explicitly to one of the isomers of Ru(dppe)(CO)₂[C(O)OMe]₂. Statements referring to both isomers will be written as the formula or as 3 and 3′.

Kinetic Analysis of the Reaction of Ru(dppe)(CO)₂[C(O)OMe]₂ with *p*-Toluidine between 75 and 103 °C. These reactions were carried out in an NMR pressure cell designed for spectroscopic studies under high gas pressures.[18] In a glovebox, stock solutions of *p*-toluidine (59.4 mM) and 3 (374 mM) were made from 5:1 toluene-*d₈*:CD₃OD. Various volumes of these solutions and pure solvent were added to the 5-mm sapphire NMR tube to give a total volume of 0.40 mL in the concentrations described in Table 1. The valve of the high-pressure tube was sealed, and the apparatus removed from the glovebox. The valve was connected to a purged stainless steel pressure line, and the cell was pressurized with CO (3 atm). The solution in the cell was shaken to insure that a reasonable amount of CO dissolved in solution, the pressure was released, and the tube was pressurized to a final pressure of 2 atm at 22 °C. The probe was heated to the desired reaction temperature, and data were collected at specific time intervals. Measurements of the concentrations of 1, 3, and 3′ were performed by integration of the ³¹P NMR spectrum.

Kinetics of the Reaction of 3 with *p*-Toluidine between 22 and 52 °C. Stock solutions of 3 and *p*-toluidine were prepared in the glovebox using a 5:1 volume/volume C₆D₆:CH₃OH solvent mixture. Various ratios of the solutions and pure solvent were added to 5-mm NMR tubes which were attached to 14/20 ground glass joints. The initial concentrations of 3 and *p*-toluidine in these solutions are listed in Table 2. The 14/20 ground glass joints were fitted with gas adapters (Teflon valves), removed from the box, frozen with liquid N₂, evacuated, and sealed using a torch. Immediately upon warming, the tube was placed in an NMR spectrometer

(15) Sanchez-Delgado, R. A.; Bradley, J. S.; Wilkinson, G. *J. Chem. Soc., Dalton Trans.* **1976**, 399.
(16) Gargulak, J. D.; Gladfelter, W. L. *Organometallics* **1994**, *13*, 698.
(17) Gargulak, J. D.; Gladfelter, W. L. *Inorg. Chem.* **1994**, *33*, 253.
(18) Roe, D. C. *J. Magn. Reson.* **1985**, *63*, 388.

with the probe warmed to the desired reaction temperature. ³¹P NMR spectra were collected at specific time intervals. The peak areas were evaluated with the integration for all species normalized to the initial concentration of 3.
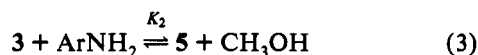
Numerical calculations for approximation of the described series of differential equations were performed using the Runge Kutta algorithm on *Mathmatica* available from Wolfram Research, Inc. The step size used in the integration was 4 min for analysis of the runs at 22 and 32 °C and 1.5 min for 42 and 52 °C. Comparison of the calculated and experimental data allowed adjustment of the values for k_1, k_{-1}, k_2, k_{-2}, k_3, k_{-3}, k_4, k_{-4}, k_5, and $k_{5'}$. The ratio of k_4 to k_{-4} was based on the experimental value of K_4, but the specific values of these forward and reverse rates were indeterminant and were input into the calculations as large numbers relative to the other rate constants.

Reaction of *p*-Tolyl Isocyanate with Various Concentrations of Aryl Amine. Five 5.0-mL solutions of *p*-toluidine in toluene and CH₃OH mixtures (5 M in CH₃OH) were prepared at the following concentrations: 9.7, 30, 45, 71, and 122 mM. To each solution in a septum-sealed vial was rapidly added 19.2 μL (0.15 mmol) of *p*-tolyl isocyanate. Each vial formed visible amounts of solid *N,N′*-ditolylurea within 5 min at ambient temperature. After 30 min the solution in each of the vials was analyzed using gas chromatography.

Thermolysis of Ru(dppe)(CO)₂[C(O)NHCH(CH₃)₂]₂ (6). An NMR tube was attached to a 14/20 ground glass joint. Ru(dppe)(CO)₂[C(O)-NHCH(CH₃)₂]₂ (5 mg) and C₆D₆ (0.5 mL) were loaded into the NMR tube in the glovebox. The tube was capped with a Teflon valve, removed from the glovebox, and sealed under vacuum. A ¹H NMR spectrum was initially collected, after which the tube was removed from the spectrometer, heated to 90 °C for 5 min, cooled in an ice bath, and reanalyzed immediately and after standing for 1.5 h.

Results

We will begin with a description of the formation and characterization of the methoxycarbonyl–carbamoyl species 5 and 5′. This will be followed by a brief description of the
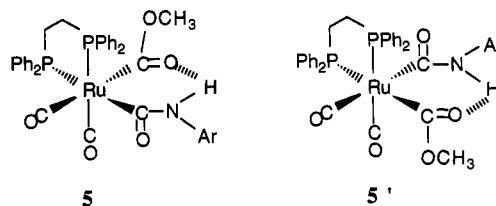
thermolysis of 6. The balance of the results section will focus on the kinetics of the reaction of 3 with ArNH₂. The kinetics outlined in this paper were conducted in two different temperature regimes, and although the final products were identical, the low-temperature regime (22–52 °C) was complicated by the appearance of intermediates 5 and 5′.

Formation and Characterization of 5 and 5′. ¹H and ³¹P NMR spectra of a CH₃OH/C₆D₆ solution of 3 and *p*-toluidine were monitored over two days. After 12 h the ³¹P NMR spectrum exhibited new resonances at 51.41 (d) and 45.76 (d) ppm (J_{PP} = 11.5 Hz) attributed to 5. The ¹H NMR spectrum collected at approximately the same time revealed resonances from 3 and 3′, CH₃OH, *p*-toluidine, and three new signals. There was a singlet at 10.78 ppm, similar in chemical shift to the hydrogen-bonded amide proton in 6;[17] a singlet located at 2.55 ppm, characteristic of the chemical shift for a methoxycarbonyl proton; and a singlet at 2.07 ppm, a shift similar to the methyl resonance from the *p*-tolyl moiety. The integration for these three signals was 1:3:3, respectively. Under identical conditions, but in the absence of CH₃OH, the formation of 1 equiv of CH₃OH was observed for every equivalent for 3 consumed. Observations of these ¹H NMR spectral signals in the methoxide and aromatic methyl regions are masked at higher concentrations of aromatic amine and CH₃OH. The reaction occurs at a much slower rate without CH₃OH as a cosolvent.

After the sample had reacted for an additional 24 h, the previously described ³¹P and ¹H resonances were still observed

Table 2. Rate Constants and Activation Parameters Derived from Numerical Analysis

T (°C)	path[a]	3[b]	ArNH₂[b]	k_1[c]	k_{-1}[c]	k_2[d]	k_{-2}[d]	k_3[d]	k_{-3}[d]	k_5[c]
22	5	0.034	0.41	0.0040	0.016	0.021	0.0033	0.0053	0.00092	0.00026
32	5	0.026	0.43	0.014	0.051	0.024	0.0044	0.010	0.0022	0.00092
42	5	0.030	0.36	0.040	0.14	0.019	0.0030	0.014	0.0035	0.0054
52	5	0.030	0.36	0.14	0.48	0.034	0.0031	0.027	0.0070	0.028
ΔH^{*}[e]	5			21.7 ± 0.7	20.7 ± 0.8	2 ± 2	−2 ± 2	9.3 ± 0.9	11.9 ± 0.9	29 ± 2
ΔS^{*}[f]	5			−4 ± 2	−4 ± 3	−69 ± 7	−83 ± 5	−45 ± 3	−40 ± 3	16 ± 6
22	5′	0.034	0.41	0.0040	0.016	0.024	0.0038	0.0057	0.00098	0.00041
32	5′	0.026	0.43	0.0145	0.052	0.029	0.0055	0.011	0.0023	0.0012
42	5	0.030	0.36	0.040	0.140	0.019	0.0042	0.015	0.0023	0.0090
52	5′	0.030	0.36	0.14	0.480	0.033	0.0065	0.032	0.0020	0.035
ΔH^{*}[e]	5′			21.6 ± 0.8	20.7 ± 0.8	0 ± 2	2 ± 2	10 ± 1	4 ± 3	29 ± 3
ΔS^{*}[f]	5′			−4 ± 2	−5 ± 3	−73 ± 8	−71 ± 6	−44 ± 4	−68 ± 10	14 ± 8

[a] All products is assumed to form through this species. [b] Initial concentration (M). [c] Units are min⁻¹. [d] Units are M⁻¹ min⁻¹. [e] Units are kcal/mol. [f] Units are eu.

as well as new signals at 57.30 (d) and 53.20 (d) ppm (J_{PP} = 13.3 Hz), indicating the presence of another asymmetric metal species. Three new resonances in the ¹H NMR spectrum at 11.14, 3.47, and 2.04 ppm (attributable to **5′**) appeared in a 1:3:3 intensity ratio. Upon standing for an additional 24 h, crystals of *N,N′-*di-*p*-tolylurea were visible in the reaction tube, and **1** was the major metal species present in the reaction solution. All attempts to isolate solid samples of **5** or **5′** were unsuccessful. The reaction of **3** with the stronger nucleophile, isopropylamine, led to immediate substitution of both methoxy groups to form the structurally characterized complex Ru(dppe)(CO)₂[C(O)NH-(*i*-Pr)]₂ (**6**).[17] The ¹H NMR spectrum of **6** displayed two signals for the amide hydrogens at 9.91 and 4.83 ppm. The large downfield chemical shift of the one hydrogen was due to the strong hydrogen bond involving the oxygen of the adjacent carbamoyl ligand. This characteristic chemical shift of the hydrogen-bonded proton was evident in both **5** and **5′**, and the structures shown above account for these observations. The stereochemistry indicated in these drawings is based on results found in the separate study of the relative rates of methoxy group exchange of **3** with methanol.[16] The methoxycarbonyl that was trans to the phosphine group underwent substitution with CD₃-OD a factor of 10 times faster than the methoxycarbonyl trans to the CO. The forward rate constants (vide infra) for converting **3** to **5** and **5′** differed by a factor of 5 (**5** forms faster) at room temperature. The assumption that the trend in substitution rates would be similar for ArNH₂ and CD₃OD allows the assignment of the structures.

Equilibrium between 3 and Aryl Amine. During the experiments described above, the concentrations of **5** and **5′** increased to a constant ratio with **3**, suggesting that equilibrium was achieved. In experiments at 22 °C similar to the above example, but in which CH₃OH concentration was increased from 1.0 to 16.2 M at constant concentration of *p*-toluidine and **3**, the reaction quotients ([5]/[3] and [5′]/[3]) decreased in a linear fashion. In a similar manner, when the *p*-toluidine concentration was varied from 0.093 to 0.86 M at constant concentrations of methanol and **3**, the same reaction quotients increased linearly. These results establish that **3**, **5**, and **5′** are connected by the equilibria shown in eqs 3 and 4. The values for K_2 and K_3 (Table 3) for the

$$3 + \text{ArNH}_2 \overset{K_2}{\rightleftharpoons} 5 + \text{CH}_3\text{OH} \qquad (3)$$

$$3 + \text{ArNH}_2 \overset{K_3}{\rightleftharpoons} 5' + \text{CH}_3\text{OH} \qquad (4)$$

temperature range from 22 to 52 °C were calculated from the specific rate constants which were determined by the method described below. The rate at which equilibrium was approached increased by a factor of 30 as the CH₃OH concentration varied from 1 to 16.2 M.

Table 3. Equilibrium Constants for Reactions Shown in Eqs 8–10 (K_1–K_3) Calculated from the Data Shown in Table 2.[a]

T (°C)	path[b]	K_1	K_2	K_3	K_4
22	5	0.25	6.4	5.8	0.30
32	5	0.28	5.5	4.6	0.41
42	5	0.29	6.3	4.0	0.45
52	5	0.29	11	3.9	0.55
ΔH[c]	5	0.9 ± 0.3	3 ± 2	−2.6 ± 0.5	3.7 ± 0.5
ΔS[d]	5	0.5 ± 0.9	15 ± 7	−5 ± 2	10 ± 2
22	5′	0.25	6.3	5.8	0.30
32	5′	0.28	5.3	4.8	0.41
42	5′	0.29	4.5	6.5	0.45
52	5′	0.29	5.1	16	0.55
ΔH[c]	5′	0.9 ± 0.3	−1.6 ± 0.9	6 ± 3	3.7 ± 0.5
ΔS[d]	5′	0.5 ± 0.9	−2 ± 3	24 ± 11	10 ± 2

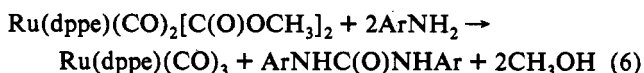[a] The values for K_4 were obtained directly from the experimental results. [b] All product assumed to form through this species. [c] Units are kcal/mol. [d] Units are eu.

Kinetics of Ru(dppe)(CO)₂[C(O)OCH₃]₂ Reacting with *p*-Toluidine from 75 to 103 °C. It was imperative that this kinetic work was done under scrupulously dry conditions. Even the smallest measurable concentrations of water caused an erroneous result due to the rapid reaction between H₂O and **3** to liberate 2 equiv of CH₃OH, CO₂, and **1** (eq 5). The concentrations were measured using ¹H and ³¹P NMR spectroscopy, and the reaction vessel was a high-pressure sapphire NMR tube.

$$\text{Ru(dppe)(CO)}_2[\text{C(O)OCH}_3]_2 + \text{H}_2\text{O} \rightarrow$$
$$\text{Ru(dppe)(CO)}_3 + 2\text{CH}_3\text{OH} + \text{CO}_2 \quad (5)$$
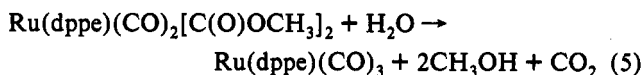
The organic product observed from the reaction of **3** (10–30 mM) with *p*-toluidine (86–700 mM) under all conditions was *N,N′-*di-*p*-tolylurea (eq 6). The urea was only partially soluble

$$\text{Ru(dppe)(CO)}_2[\text{C(O)OCH}_3]_2 + 2\text{ArNH}_2 \rightarrow$$
$$\text{Ru(dppe)(CO)}_3 + \text{ArNHC(O)NHAr} + 2\text{CH}_3\text{OH} \quad (6)$$

in the reaction solution and crystallized upon cooling. The stoichiometry was quantified using ¹H NMR spectral integration of the aryl methyl group before the urea began to crystallize. Yields greater than 95% were commonly calculated for these reactions.

Table 1 lists the results, and Figure 1 displays a series of ³¹P NMR spectra collected for a typical experiment. The reaction was complete within 66 min at 95 °C at the following concentrations: **3**, 29.7 mM; ArNH₂, 196 mM. *No other species except 3′ and 1 were observed in these spectra.* The effects of varying concentrations of **3** and *p*-toluidine on the initial rate of the reaction
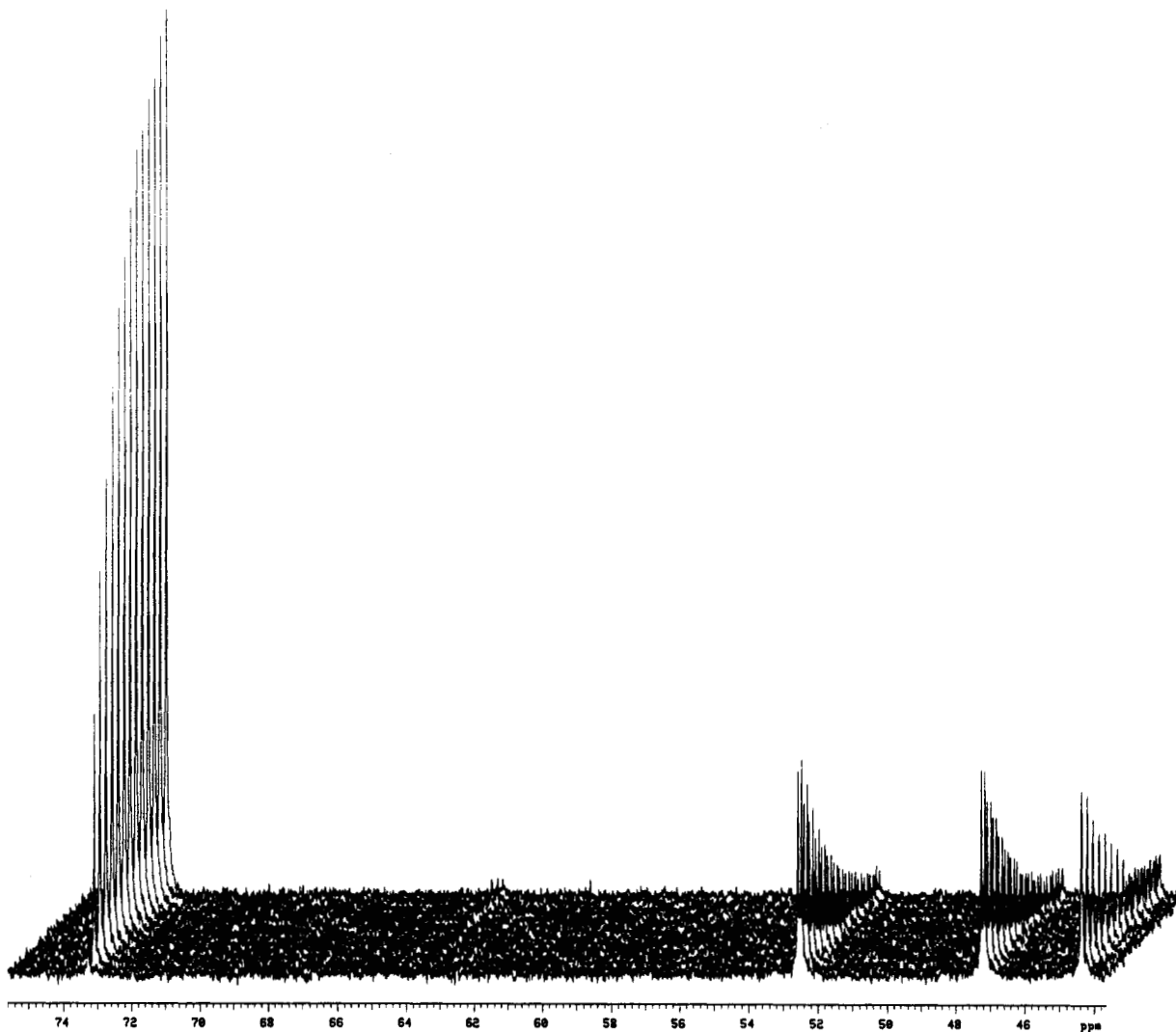
Figure 1. ^{31}P NMR spectra collected as a function of increasing time (going into the page) at 75 °C showing the disappearance of **3** (doublets at 46 and 52 ppm) and **3'** (singlet at 43 ppm) and the formation of **1** (singlet at 73 ppm).
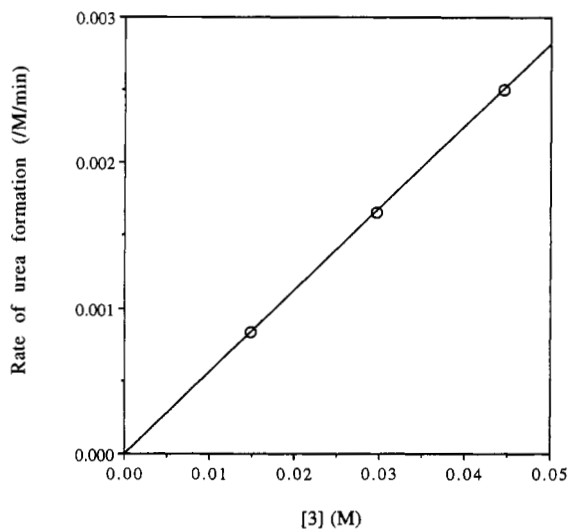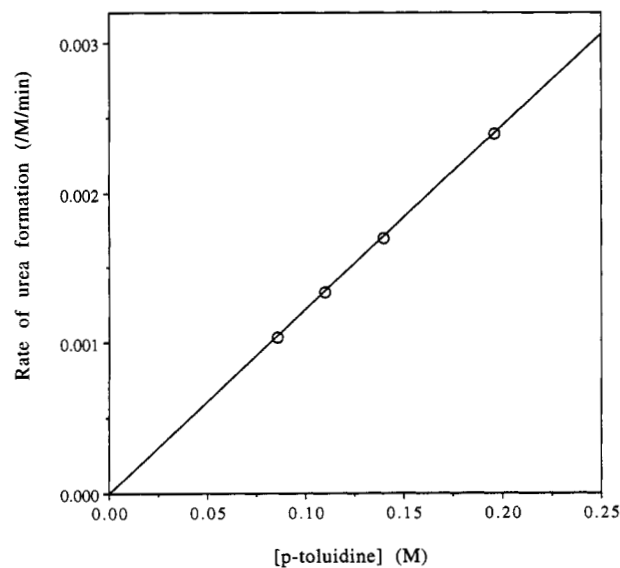

Figure 2. Initial rate of urea formation from the reaction of **3** with *p*-toluidine at 95 °C. A first-order dependence is shown with respect to the concentration of the metal complex.


Figure 3. Initial rate of urea formation from the reaction of **3** with *p*-toluidine at 95 °C. A first-order depenendence is shown with respect to the concentration of *p*-toluidine.

(defined as the first four data points) are shown in Figures 2 and 3, respectively. The observed rate constants listed in Table 1 were determined by the best fits of the rate law (eq 7) to the experimental data taken out to three half lives.

Reaction of 3 and *p*-Toluidine between 22 and 52 °C. As described above, two isomeric carbamoyl–methoxycarbonyl complexes were observed during the reaction of **3** with $ArNH_2$

$$\text{rate} = k_u[\text{ArNH}_2]\{\text{Ru(dppe)(CO)}_2[\text{C(O)OCH}_3]_2\} \quad (7)$$

between 22 and 52 °C. The concentration profile for a reaction at 22 °C is displayed in Figure 4. The concentrations were based on integration of the ^{31}P NMR spectral signals of each species in solution after normalizing the integral for the total area to the initial concentration of 3. Analysis of the proton spectra for the same reaction was not possible because the high aryl amine concentration required to see appreciable 5 and 5′ masked the fine details needed to determine accurately the concentration of 5 and 5′. No other signals were observed in the ^{31}P NMR spectrum except those described below.

During the initial 150 min of the reaction at 22 °C, consumption of 3 and 3′ occurred, and 5 reached equilibrium with 3 (eq 3). On a longer time scale, 5′ also increased in concentration. Slow, near-linear formation of 1 was observed during the reaction, starting at a concentration slightly higher than zero. The non-zero initial concentration of 1 was due to a small amount of decomposition of 3 which occurred before mixing of the reagents. For each run the value was determined and used for the initial concentration of 1 in the kinetic expression.

As the concentration of 5′ increased, a singlet at 53.3 ppm in the ^{31}P NMR spectrum became visible. Its intensity was always small, typically one-third that of the signal due to 5′. The singlet requires that both the phosphines are equivalent, and the chemical shift is very close to those of 5 and 5′. A similar signal was observed during the reaction of 3 with isopropylamine.[17] Although both structures, 8 and 9, are consistent with these data, the

8   9
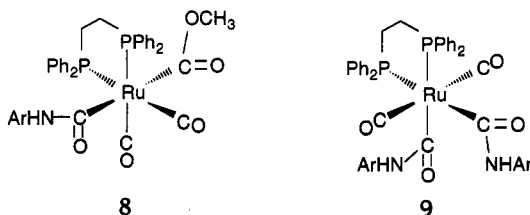
apparant connection between the concentration of 5′ and this new species at all amine concentrations suggests that 8 (an isomer of 5′ and, therefore, 5) is the more likely of the two structures. The isomerization of 3 to 3′ occurs by an intramolecular "ligand-hopping" of the methoxy group from one CO to another.[16] The formation of 8 by the analogous event could occur directly from 5′, but not from 5.

Kinetics of 3 and *p*-Toluidine between 22 and 52 °C. During the formation of 5 and 5′ from 3 in the determination of the effects of CH$_3$OH and *p*-toluidine concentrations on K_2 and K_3, it was observed at ambient conditions that 5 achieved equilibrium much faster than 5′ and that their relative concentrations decreased with time, resulting in the stoichiometric formation of urea and 1. Equations 8–11 depict the reactions occurring in

$$3 \underset{k_{-1}}{\overset{k_1}{\rightleftharpoons}} 3' \quad (8)$$

$$3 + \text{ArNH}_2 \underset{k_{-2}}{\overset{k_2}{\rightleftharpoons}} 5 + \text{CH}_3\text{OH} \quad (9)$$

$$3 + \text{ArNH}_2 \underset{k_{-3}}{\overset{k_3}{\rightleftharpoons}} 5' + \text{CH}_3\text{OH} \quad (10)$$

$$5' \underset{k_{-4}}{\overset{k_4}{\rightleftharpoons}} 8 \quad (11)$$
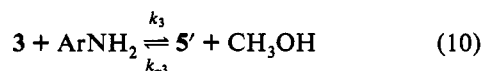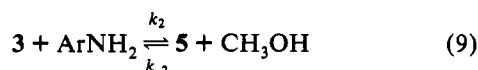
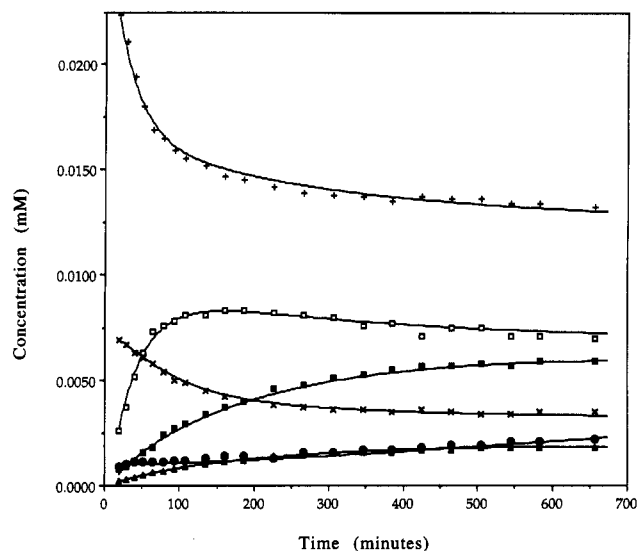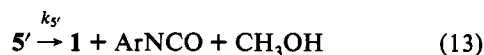solution. A scenario where 5 or 5′ could be responsible for product formation through a unimolecular reaction is illustrated in eqs

Figure 4. Experimental data and theoretical model for the progress of reaction of 3 with *p*-toluidine at 22 °C: +, [3]; ×, [3′]; □, [5]; ■, [5′]; △, [8]; ● [1]. Fits of similar quality were obtained for all four temperatures studied involving either 5 or 5′ as the product forming intermediate. The solution shown in this figure assumes that all product forms from 5.

12 and 13. The aryl isocyanate would be rapidly trapped by any

$$5 \xrightarrow{k_5} 1 + \text{ArNCO} + \text{CH}_3\text{OH} \quad (12)$$

$$5' \xrightarrow{k_{5'}} 1 + \text{ArNCO} + \text{CH}_3\text{OH} \quad (13)$$

free aryl amine in the solutions. On the basis of the above equilibria (eqs 8–11) and the unimolecular decomposition of 5 (eq 12), the following set of rate equations and the ruthenium mass balance (eqs 14–20) can be written. Numerical integration

$$d[3]/dt = -\{k_2 + k_3\}[\text{ArNH}_2][3] - k_1[3] + k_{-1}[3'] + \\ k_{-2}[\text{CH}_3\text{OH}][5] + k_{-3}[\text{CH}_3\text{OH}][5'] \quad (14)$$

$$d[3']/dt = k_1[3] - k_{-1}[3'] \quad (15)$$

$$d[5]/dt = k_2[\text{ArNH}_2][3] - k_5[5] - k_{-2}[\text{CH}_3\text{OH}][5] \quad (16)$$

$$d[5']/dt = k_3[\text{ArNH}_2][3] - k_4[5'] - \\ k_{-3}[\text{CH}_3\text{OH}][5'] + k_{-4}[8] \quad (17)$$

$$d[1]/dt = k_5[5] \quad (18)$$

$$d[8]/dt = k_4[5'] - k_{-4}[8] \quad (19)$$

$$[\text{Ru}]_{\text{total}} = [3] + [3'] + [5] + [5'] + [1] + [8] \quad (20)$$

of this series of differential equations using the Runge Kutta method was successful. The mass balance for Ru species (eq 20) was implicit and was based upon the initial concentrations. The calculated curves in Figure 4 are based on this numerical integration. Using this model, the individual rate constants were determined and are displayed in Table 2. Good sensitivity was obtained for these fits, with errors on individual k values assigned as ±10% on the basis of the fact that deviations of this magnitude for any one constant caused considerable skewing of the model from the experimental data. The alternative procedure, in which 5′ was the productive intermediate, involved suitable changes to eqs 16–18 and gave similar values for the rate constants (Table 2). Table 3 shows the values of K_1, K_2, and K_3 calculated from 22 to 52 °C using the data from Table 2. The values shown for

Homogeneous Catalytic Carbonylation of Nitroaromatics

J. Am. Chem. Soc., Vol. 116, No. 9, 1994 3797

K_4 were calculated from the ratios of **8** to **5'** obtained directly from the spectra.

Reactivity of 6. Thermolysis of a 14 mM solution of **6** for 5 min at 90 °C in C_6D_6 in a sealed NMR tube under vacuum resulted in a 1.8:1.2:0.2 ratio of diisopropylurea (4.2 ppm, overlapping d and m, 2H; 1.1 ppm, d, 6H):isopropylamine (2.9 ppm, m, 1H; 0.95 ppm, d, 6H):isopropyl isocyanate (3.0 ppm, m, 1H; 0.75 ppm, d, 6H). Upon standing for 1.5 h, the residual isopropyl isocyanate was consumed, and a 2.3:1 ratio of diisopropylurea to isopropylamine was observed. The conversion of **6** to **1** was 80%, and no other metal species were observed in the ^{31}P NMR spectrum. The net reaction is shown in eq 21. This

$$6 \rightarrow \{1 + RNCO + RNH_2\} \rightarrow 1 + (RNH)_2CO \quad (21)$$
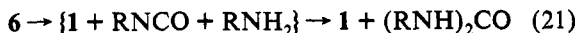
experiment was attempted at higher concentrations of **6** (50 mM), but rapid urea formation masked direct observation of the isocyanate. The nonstoichiometric conversion to urea evidenced by the presence of excess amine was probably due to trace amounts of water which could react with the isopropyl isocyanate to form amine and CO_2.

Reaction of *p*-Tolyl Isocyanate with *p*-Toluidine. Toluene solutions of *p*-toluidine and methanol (4.8 M in CH_3OH) were reacted with *p*-tolyl isocyanate at various concentrations to probe the selectivity of urea vs methyl *N*-*p*-tolylcarbamate formation. Even when the ratio of amine to CH_3OH was 1 to 160 and the amount of isocyanate added was slightly below a stoichiometric concentration with respect to the amine, only *N*,*N'*-di-*p*-tolylurea was formed. No evidence for formation of carbamate was found by GC analysis until the ratio of amine to isocyanate dropped below stoichiometric. (0.5:1).

Discussion

Before detailing the chemistry occurring between Ru(dppe)-$(CO)_2[C(O)OMe]_2$ and amines, it is worth briefly reviewing the reactivity of this unusual bis(methoxycarbonyl) complex. The two isomers, **3** and **3'**, interconvert by an intramolecular "ligand-hopping" mechanism in which a methoxy group migrates from a methoxycarbonyl to an adjacent metal carbonyl ligand. The primary coordination sphere of this octahedral, d^6, Ru^{2+} complex is inert toward substitution on the time scale of all the reactions discussed in this paper. Only 10% of the carbonyls exchanged with ^{13}CO (3 atm) following 3 weeks of reaction at room temperature. The ester-like functional groups do undergo a transesterification upon reaction with other alcohols. Kinetic studies of the exchange of isomer **3** with CD_3OD at 21 °C established that the rate of substitution of the methoxycarbonyl located trans to the phosphine was an order of magnitude higher (0.48 M^{-1} min^{-1}) than the rate of substitution of the group located trans to CO (0.048 M^{-1} m^{-1}). All OCD_3 incorporation into isomer **3'** was accounted for by the rate of isomerization, leading to the conclusion that **3'** is inert (relative to **3**) toward substitution of the methoxy groups. The mechanism of methoxy group exchange of **3** that is most consistent with the experimental data involves initial nucleophilic attack of the methanol on one of the metal carbonyl ligands.[16]

The reaction of Ru(dppe)$_2$(CO)$_2$[C(O)OCH$_3$]$_2$ with aryl amines occurs relatively rapidly at room temperature. Within 150 min, the equilibrium concentration of the new monosubstituted complex, Ru(dppe)$_2$(CO)$_2$[C(O)OCH$_3$][C(O)NHAr], forms. At longer times, this complex undergoes unimolecular reaction to form Ru(dppe)(CO)$_3$, aryl isocyanate (trapped immediately by the excess amine), and methanol. This relatively simple scheme, eqs 22 and 23, is complicated by the additional equilibria involving
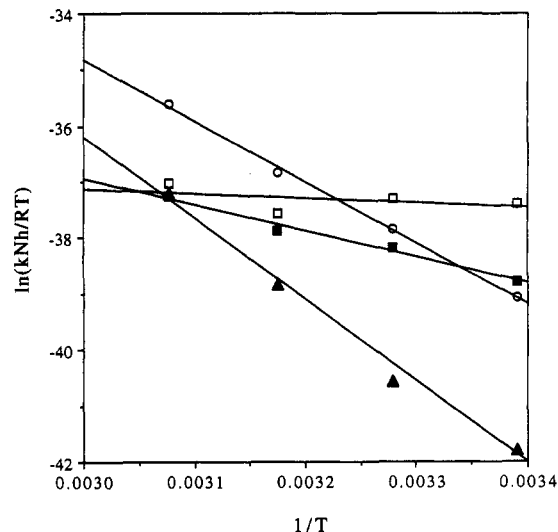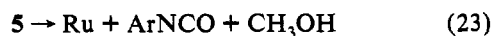
$$3 + ArNH_2 \rightleftharpoons CH_3OH + 5 \quad (22)$$

$$5 \rightarrow Ru + ArNCO + CH_3OH \quad (23)$$

Figure 5. Eyring plot for k_1 (O), k_2 (□), k_3 (■), and k_5 (▲).

3. This includes the isomerization of **3** to the less reactive (toward substitution) molecule, **3'**, and the reaction of aryl amine with **3** to give the isomeric, monosubstituted complex **5'**. This latter species can also produce the products of the reactions.

The numerical integration procedure used to determine the specific rate constants gave excellent fits to the experimental data at all temperatures studied. In addition, the rate constants produced linear Eyring plots as exemplified for k_1, k_2, k_3, and k_5 in Figure 5. An independent check on the procedure was possible by comparing the rate constants, k_1 and k_{-1}, for isomerization of **3** obtained by the numerical fit to the analogous rates obtained[16] for this isomerization as it occurs in the absence of $ArNH_2$ and methanol. Although the conditions of these two experiments differed with regard to the methanol concentration (5 vs 0 M), the values of k_1 differed by only 7%.

We were fortunate to be able to study this system by starting with samples of pure Ru(dppe)(CO)$_2$[C(O)OCH$_3$]$_2$ because the evaluation of the kinetics *during the approach to equilibrium* allowed a unique determination of the rates of most of the reactions. In the following sections we will discuss separately the results that allow the determination of the mechanisms of the N–C bond forming step and the subsequent formation of the product. In some of the possible mechanisms, both N–C bond formation and product formation occur simultaneously.

C–N Bond Forming Step. Scheme 1 outlines the reasonable mechanisms that could lead to C–N bond formation. Both the reductive elimination and the migratory insertion mechanisms require the prior coordination of the aryl amide ligand. The formation of this moiety from Ru(dppe)(CO)$_2$[C(O)OCH$_3$]$_2$ would require formation of a vacant site by CO dissociation or dissociation of one end of the chelating phosphine ligand. Both of these possibilities (and as a result both the reductive elimination and migratory insertion mechanisms) can be dismissed because (1) there is no dependence of the rate on the pressure of CO (up to at least 3 atm) and (2) the rate of exchange of ^{13}CO with Ru(dppe)(CO)$_2$[C(O)OCH$_3$]$_2$ is far slower than the rate of $ArNH_2$ reaction with Ru(dppe)(CO)$_2$[C(O)OCH$_3$]$_2$. In addition, the reductive elimination mechanism would produce carbamate directly rather than the observed product, diarylurea.
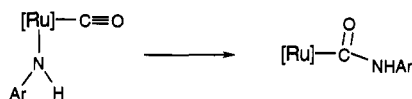
Nucleophilic attack of the aryl amine on the complex could lead to displacement of the metal with direct formation of the product or to formation of the intermediate carbamoyl ligand. The former mechanism is ruled out because it would produce the wrong product, a carbamate. The formation of the carbamoyl ligand by nucleophilic attack on a metal carbonyl or on a methoxycarbonyl cannot be dismissed by any of our data. Unfortunately the site of nucleophilic attack cannot be established

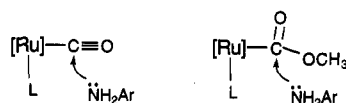**Scheme 1.** Possible Mechanisms for Carbon–Nitrogen Bond Formation

a. Reductive Elimination

$$[Ru]-C(O)OCH_3, \ N(Ar)(H) \longrightarrow [Ru] + ArNHC(O)OCH_3$$
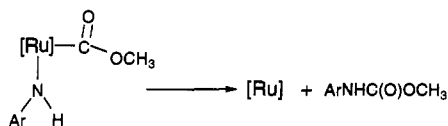
b. Migratory Insertion

$$[Ru]-C\equiv O, \ N(Ar)(H) \longrightarrow [Ru]-C(O)NHAr$$

c. Nucleophilic Attack on a Coordinated Ligand

$$[Ru]-C\equiv O, \ L, \ \ddot{N}H_2Ar \qquad [Ru]-C(O)OCH_3, \ L, \ \ddot{N}H_2Ar$$

by our kinetics or any of our direct evidence. In a separate study of the transesterification of $Ru(dppe)(CO)_2[C(O)OCH_3]_2$, the reactivity patterns could be best explained by invoking nucleophilic attack on a metal carbonyl.[16] It is reasonable to expect a similar mechanism of nucleophilic attack with the aryl amine.

We conclude that the C–N bond forming step in the reaction between $Ru(dppe)(CO)_2[C(O)OCH_3]_2$ and aryl amines occurs by a nucleophilic attack and that this attack is probably directed at a metal carbonyl. The activation parameters (Table 2) calculated for this reaction exhibit large, negative entropies of activation. The magnitude of these values are somewhat larger than those observed for the attack of nucleophiles such as methoxide[19] and trimethylamine N-oxide[20] on $Ru(CO)_5$. This may be due to more stringent steric constraints or to a greater contribution from change in solvent ordering in the transition state for the more polar structure of $Ru(dppe)(CO)_2[C(O)-OCH_3]_2$. It is also possible that more than a single microscopic step is involved in the equilibria represented by eqs 9 and 10 and that k_2 and k_{-2} (and k_3 and k_{-3}) represent a convolution of specific rate constants. Comparing this reaction to the mechanism of hydrolysis or amination of organic esters would lead one to expect a more complicated scheme which ultimately must account for all of the proton-transfer steps. The increase in the rate of approach to equilibrium for eqs 9 and 10 as the methanol concentration is increased is consistent with a picture where the more polar solvent mixture enhances the rate of proton-transfer steps.
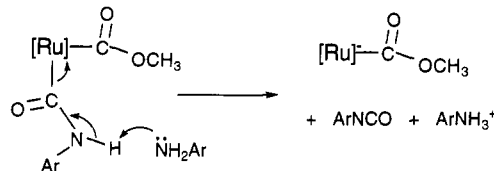
Product Forming Step. Scheme 2 outlines several reasonable mechanisms for removing the organic product from the catalyst. Although the reactivity of carbamoyl ligands has not been widely studied, one of the early reports of their behavior describes the elimination of isocyanate caused by deprotonation with triethylamine (eq 24).[21] The analogous elimination from $Ru(dppe)(CO)_2$-
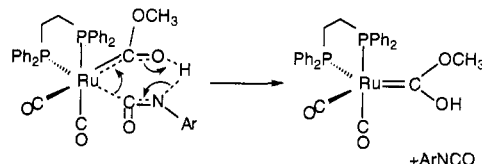
$$CpW(CO)_3[C(O)NHMe] + Et_3N \longrightarrow$$
$$MeNCO + [CpW(CO)_3]^- + [Et_3NH]^+ \quad (24)$$
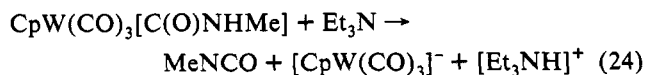
$[C(O)OCH_3][C(O)NHAr]$ involving $ArNH_2$ as the external base is a possible mechanism of product formation. It can,
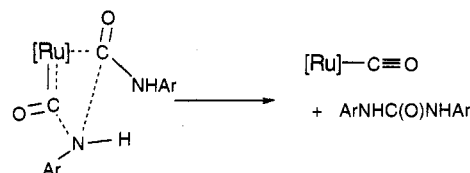
Scheme 2. Possible Product Forming Steps

a. Intermolecular Elimination

$$[Ru]-C(O)OCH_3, \ O=C-N(Ar)(H), \ \ddot{N}H_2Ar \longrightarrow [Ru]-C(O)OCH_3 + ArNCO + ArNH_3^+$$

b. Intramolecular Elimination

$$Ph_2P, PPh_2, Ru, OCH_3 \ldots \longrightarrow Ph_2P, PPh_2, Ru=C(OCH_3)(OH) + ArNCO$$

c. Cycloreversion

$$[Ru]-C(O)(NHAr), \ O=C-N(Ar)(H) \longrightarrow [Ru]-C\equiv O + ArNHC(O)NHAr$$

however, be dismissed because it would require the overall conversion from $Ru(dppe)(CO)_2[C(O)OCH_3]_2$ to products to exhibit second-order kinetics with respect to the concentration of $ArNH_2$. This transformation is cleanly first order in $ArNH_2$.

The intramolecular elimination of aryl isocyanate is consistent with the observed kinetics, and the structure of $Ru(dppe)(CO)_2$-$[C(O)OCH_3][C(O)NHAr]$ is ideally posed to undergo this reaction. Although this mixed methoxycarbonyl–carbamoyl complex could not be isolated, its ^1H NMR spectrum exhibited a downfield shift of the amido hydrogen characteristic of a hydrogen bond to the oxygen of the methoxycarbonyl ligand. The X-ray crystallographic study of the bis(carbamoyl) complex, $Ru(dppe)(CO)_2[C(O)NH-i-Pr]_2$, identified the details of this hydrogen-bonded six-membered ring.[17] This complex eliminates isopropyl isocyanate and isopropylamine upon thermolysis, providing excellent precedent for the reactions of 5 and 5′. A concerted rearrangement illustrated in Scheme 2 allows the expulsion of aryl isocyanate and leaves a hydroxy–methoxy carbene which would readily lose methanol and form $Ru(dppe)$-$(CO)_3$. The slightly positive values for activation entropy can be understood because the ground-state structures of 5 and 5′ are already organized in a constrained arrangement that can lead to the products.

The last possible mechanism for removal of the organic product shown in Scheme 2 is referred to as a cycloreversion. Regardless of whether this is proposed to occur from 5 or 5′ or even a bis-(carbamoyl) complex, 9, direct experimental evidence rules out this mechanism. Cycloreversion from 5 or 5′ would lead directly to carbamate, the wrong product, and cycloreversion from 9 would require second-order kinetics with respect to the concentration of aryl amine.

We conclude that the intramolecular elimination of aryl isocyanate is the mechanism which releases the organic product from the catalyst. In all of the stoichiometric reactions, this isocyanate is immediately trapped by $ArNH_2$ to form the observed product, diarylurea. When the reaction was conducted under catalytic conditions, either diarylurea or the carbamate was observed depending upon the conditions. Even in those runs that produced carbamates, urea was still proposed to be the intermediate.[6]

(19) Trautman, R. J.; Gross, D. C.; Ford, P. C. *J. Am. Chem. Soc.* **1985**, *107*, 2355.
(20) Shen, J.-K.; Gao, Y.-C.; Basolo, F. *Organometallics* **1989**, *8*, 2144.
(21) Jetz, W.; Angelici, R. J. *J. Am. Chem. Soc.* **1972**, *94*, 3799.
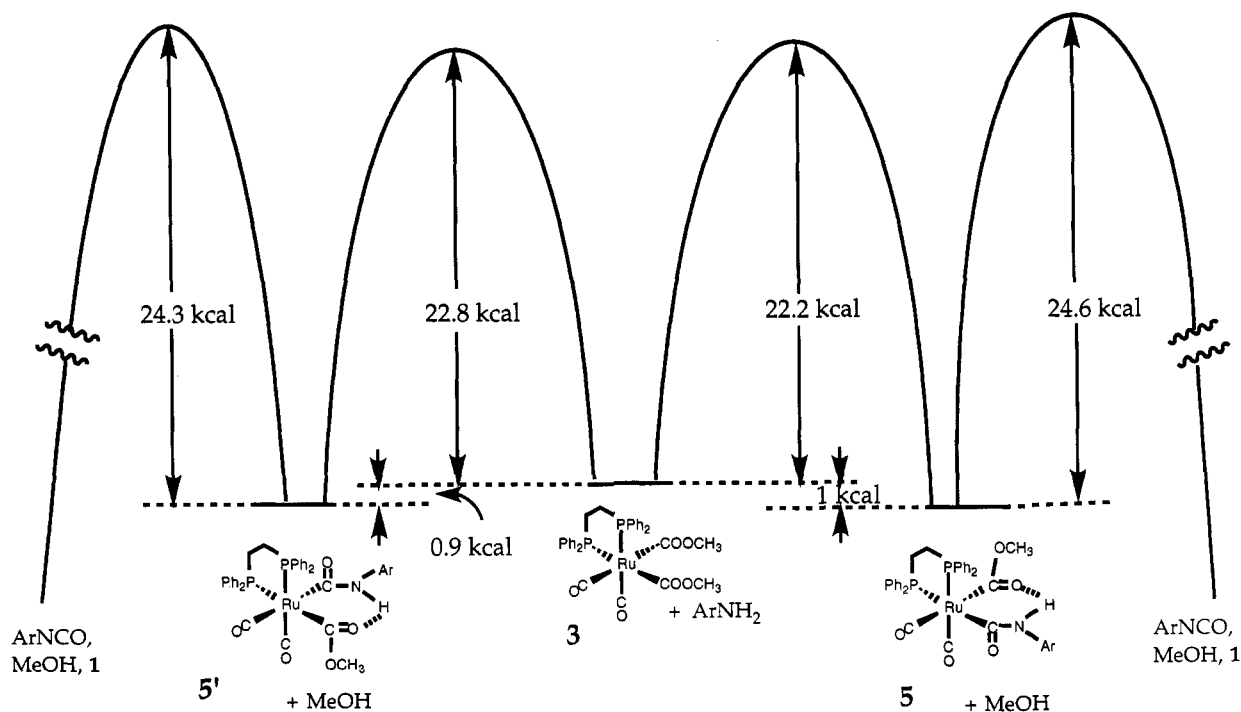
Figure 6. Energy level diagram for the transformations of **3** to products. The equilibrium between **3** and **3'** is not shown. The values are calculated at 22 °C, and the standard states of the components are 1 M.

The results discussed in this and the preceding section can be effectively summarized on the reaction coordinate diagram shown in Figure 6, where the values of free energy were calculated using a temperature of 22 °C and the standard state concentration of 1 M. The equilibria between **3** and $ArNH_2$ are represented with one barrier even though these reactions involve several microscopic proton-transfer steps in addition to the nucleophilic attack and cleavage of the C–O bond. Recall that **5** and **5'** are isomers of each other so that their similar reactivity is not surprising. It is worth reiterating that, in the determination of the rate constants for the conversion of **5** to products, we ignored the reaction of **5'** to products. Likewise the rate constant involving **5'** was obtained by shutting down product formation from **5**. Both of the mechanisms gave equally good fits to the experimental results, and we would expect to be able to fit the data with any linear combination (e.g., 30% of the product forms from **5** and 70% from **5'**) between the two extreme cases. We believe that the similarities in the reaction coordinate diagram, despite the fact that the numbers were determined for the extreme cases, indicate that both isomers contribute to product formation.

Comparison of the Kinetics of the Stoichiometric Reactions to the Catalytic Kinetics. The catalytic carbamate formation follows the empirical rate law shown in eq 25, where $[Ru_t]$ represents the

$$\text{rate} = k_c[ArNH_2][Ru_t] \qquad (25)$$

concentration of $Ru(dppe)(CO)_3$ initially charged to the reactor.[12] The observed rate constant, k_c, was evaluated at temperatures from 125 to 165 °C. The study of the stoichiometric reaction between $Ru(dppe)(CO)_2[C(O)OCH_3]_2$ and $ArNH_2$ from 72 to 103 °C established the rate law shown in eq 7. The *in situ* spectroscopic studies of the high-pressure catalysis established that the principal species observed in solution was $Ru(dppe)$-$(CO)_2[C(O)OCH_3]_2$, a fact that allows a direct comparison between the observed rate constants in eqs 7 and 25. Although linear Arrhenius behavior for a complex kinetic system is not required, we do observe a straight line (Figure 7), which establishes that both data sets represent the same process.

The stoichiometric studies of the reaction of $Ru(dppe)(CO)_2$-$[C(O)OCH_3]_2$ with $ArNH_2$ from 22 to 52 °C indicated that
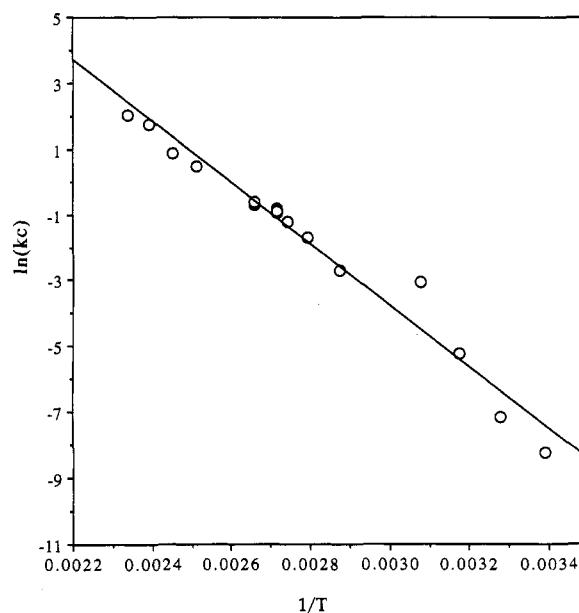

Figure 7. Arrhenius plot of k_{obs} from 22 to 165 °C. The rates plotted for the actual catalysis (from 125 to 165 °C) and those plotted for the stoichiometric reaction from 75 to 103 °C were obtained directly from the experimental data. The values plotted in the range from 22 to 52 °C were calculated using eq 26 and the experimental specific rate constants determined in this study and assume that all product forms from the intermediate **5**.

several intermediate steps were involved in this conversion. Assuming that the equilibria will be rapid at the higher temperatures, we can derive a catalytic rate expression based on the microscopic steps studied in this paper. Equation 26 is derived

$$\text{rate} = \frac{k_5 K_2[Ru_t][ArNH_2]}{[MeOH](1 + K_1) + [ArNH_2](K_2 + K_3 + K_3 K_4)} \qquad (26)$$

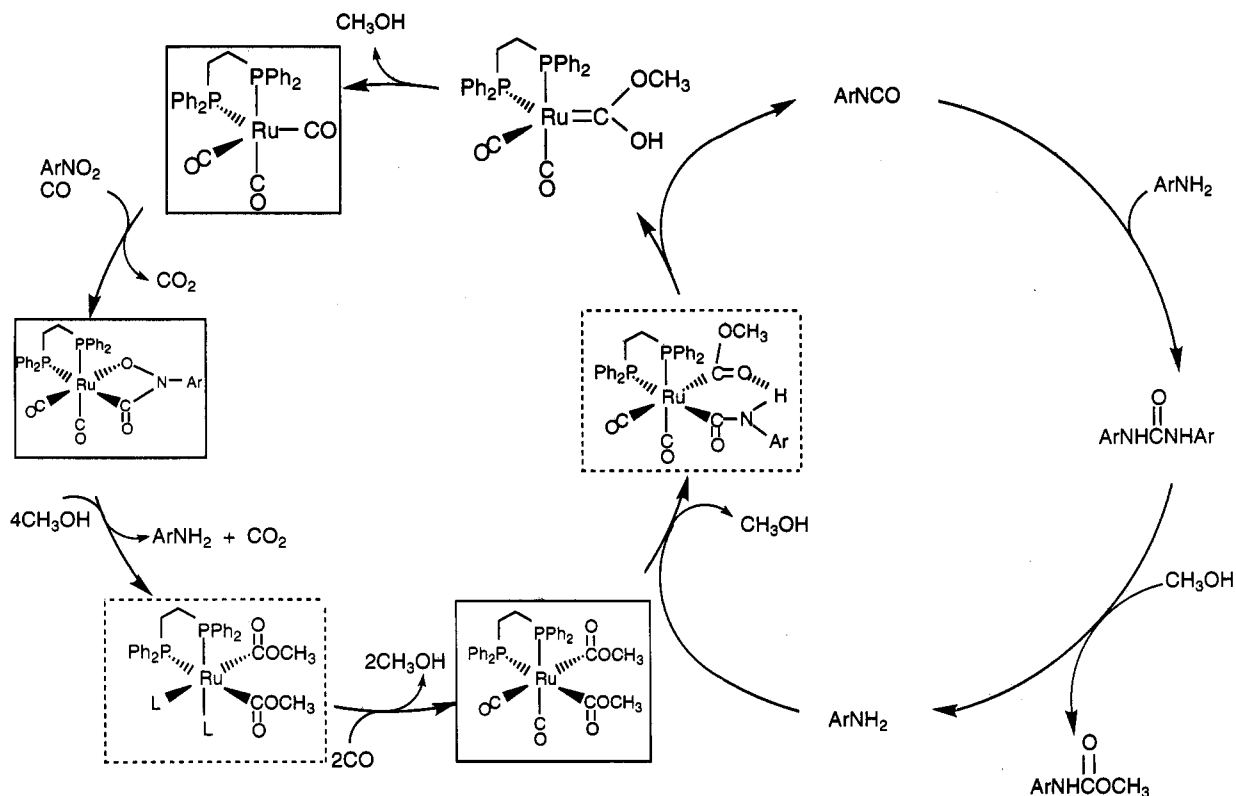from the equilibria and rates represented by eqs 8–12 and a mass

Figure 8. Summary of the mechanism of the overall catalytic cycle. The ruthenium complexes within solid boxes have been isolated and fully characterized. Those within dashed boxes have been observed but neither fully characterized nor isolated. The identities of the two ligands, labeled L, in the precursor to 3 remain obscure. The hydroxymethoxycarbene has not been observed.

balance equation for the ruthenium complexes, 3, 3', 5, 5', and 8. This expression assumes that all of the product forms via the intermediate 5, and it predicts that the rate of catalysis should saturate at high aryl amine concentrations. Unfortunately, in our earlier study, we were prohibited from raising the amine concentration above 0.052 M because the crystallization of diarylurea interfered with our analysis. Equation 26 also predicts an inverse dependence of the rate on the methanol concentration. At the lowest methanol concentration studied, 1.2 M, the catalytic rate increased by nearly 50% over the rate observed at 2.6 M. Equation 27 relates the observed catalytic rate constant, k_c, to an

$$k_c = \frac{k_5 K_2}{[\text{MeOH}](1 + K_1) + [\text{ArNH}_2](K_2 + K_3 + K_3 K_4)} \quad (27)$$

expression that can be calculated and added to the Arrhenius plot shown in Figure 7. Because the catalytic reaction rates plotted in Figure 7 were obtained at concentrations of methanol and aryl amine of 5 and 0.005 M, respectively, the second term in the denominator did not contribute significantly to the expression.[12] The agreement displayed in Figure 7 is remarkable considering the large difference in temperature between the catalytic and stoichiometric studies. The temperature (52 °C) that exhibited the greatest deviation contained the fewest data points in the critical approach-to-equilibrium regime. This regime was found to be most important for determining the values of k_2 and k_3 accurately. It seems less likely, but not impossible, that the steeper slope defined by the four data from 22 to 52 °C could be indicative of a change in the rate determining step.

Summary

In this paper we have identified that two isomers of Ru(dppe)-(CO)$_2$[C(O)OCH$_3$][C(O)NHAr] are in equilibrium with Ru-(dppe)(CO)$_2$[C(O)OCH$_3$]$_2$ and ArNH$_2$ and have established that the mechanism of C–N bond formation involves nucleophilic attack of ArNH$_2$ on a metal carbonyl. Either or both of these intermediates undergo a unimolecular elimination of aryl isocyanate which is rapidly trapped to give the products of the catalysis. By measuring the rates and equilibria of the stoichiometric reactions at several temperatures, we can predict the concentrations of the species in solution and the rate at which they form products during that actual catalytic process. The agreements with the *in situ* infrared spectroscopic studies[12] showing that Ru(dppe)(CO)$_2$[C(O)OMe]$_2$ is the major species present in solution and with the observed catalytic rates are excellent. This constitutes the determination of the mechanism of the rate (or turnover) limiting portion of the catalytic cycle using Ru(dppe)(CO)$_3$. Figure 8 incorporates the details into a summarized catalytic cycle.

Unanswered questions about the catalytic cycle remain, especially regarding the early stages. Work is continuing that focuses on the mechanism of the activation of the starting nitroaromatic and the mechanism of cleavage of the N–O bonds.